A novel correction algorithm for PTV

Yerbol K. Akhmetbekov[2], Dmitriy M. Markovich[1,2] *, Mikhail P. Tokarev[2]

1: *Institute of Thermophysics, Siberian Branch of RAS, Lavrentyev Ave. 1, Novosibirsk, 630090, Russia*
2: *Novosibirsk State University, Pirogova str., 2, Novosibirsk, 630090, Russia*

Tel: +7 383 3309040

Fax: +7 383 3356684

Email: dmark@itp.nsc.ru

Abstract

Present work announces a novel algorithm based on paired particles images correlation correction. The proposed correction assumes a new step between displacement vector formation and outlier vectors detection to be taken. The impact of a particle image diameter, particles concentration and displacement value on correction accuracy is studied using artificially generated particles images. The performance of correction is investigated during processing of experimentally obtained data. The influence of the correction on the locality of the PTV is analyzed. The merit of proposed correction is that it might be employed as a correction after PIV/PTV hybrid methods as well as after pure PTV.

1
Introduction

Modern particle imaging techniques are based on two main approaches: cross-correlation analysis of the particle images acquired with certain time delay (Particle Image Velocimetry) and individual particle tracking algorithm (Particle Tracking Velocimetry). PIV method is widely spread and thoroughly studied. However, to achieve better spatial resolution PTV method is considered to be more suitable.

The process of irregular velocity field calculation by PTV method in general includes the following steps: particle identification, particles pair matching and displacement vector calculation, spurious vectors elimination. The main problems inherent to PTV are the detection of shaded and overlapped particles and a low precision of the determination of particle center position. The first issue leads to decreasing of total amount of vectors in resulted velocity field and increasing the portion of outliers, hence the spatial resolution decreases eliminating the method's merits. Accuracy in determination of particles center positions is a crucial point in high order statistical moments calculation which is essential for profound study of a physical object.

Reported by Etoh T. et al. (1998) particle image with Gaussian mask correlation method (Particle mask correlation – PMC) provides essential improvement of the PTV ability in robust particle detection, comparing to the frequently used method of a simple brightness threshold binarization. PMC method retrieves particles images on the basis of their similarity to two-dimensional Gaussian brightness distribution, ignoring absolute peak brightness value. Normalized correlation coefficients for image portion surrounding the current pixel with preliminary estimated Gaussian mask are calculated for each point, producing correlation field. The correlation field is binarized with certain threshold and correlation field peak is detected in arisen domains. This peak corresponds to the particle position. The method also automatically identifies overlapped particle images.

Relaxation method was used for crucial step of particles pair matching. This method developed by Baek S.J. et al. (1996) is based on valuation of pairs' probabilities. Method is based on iterative passing through possible pair candidates. Each candidate has initial correctness probability besides there is separate probability for pair loss. Pairs are populated within the certain area of maximum possible particle displacement. Calculated on the previous iteration step probabilities of neighboring particles pairs which perform approximately the same displacement as current one contribute to the current pair probability. This method has strong ability to recover particles pairs without any preliminary calculations and can be applied to flows with high seeding density (up to 0.05 particles/pix^2). However, described above method is time consuming. Preliminary calculated data can greatly reduce the candidates' number and boost method performance.

Present work announces a novel correction over particle image correlation algorithm to overcome the lack of accuracy of the PTV. Using the correction one could gain both the spatial resolution and accuracy. This work intends to study the characteristics of the method.

2

The PTV algorithm

Scheme of the PTV algorithm with correction is presented in Fig. 1. It consists of the four main steps: particles center position detection, particle tracking, proposed displacement correction and outliers' detection.

2.1

Particles pairing

The performance of relaxation method mentioned above has been improved through using preliminary calculated PIV data. Let us call it Hybrid Relaxation method in this paper. Original method has several parameters. First of them is maximum possible displacement T_m. Pair candidates are considered within this radius in the second frame. The second parameter T_n designates the radius of the current particle neighborhood. All neighboring particles should perform almost the same displacement with a little deviation. The maximum permitted value of that deviation is third parameter called T_q.

PIV data obtained by the previous step can be used in different ways. One may just consider the nearest particle to the predicted point as pair. This method is called super – resolution PIV and worth its name. It is PIV with extension, hence this method has all drawbacks of the PIV not being able to recover high velocity gradients and small-scale structures. In our study we used Relaxation PTV method. The main task was only to narrow the number of candidates eliminating obviously spurious pairs. So hybrid method has three more parameters and there is no more need in T_m. All of new parameters concern the radius of the area in the second frame to search for pair. The main parameter is the ratio between the searching area radius and predicted velocity vector length, which was interpolated in the current particle center. Other two are the minimum and maximum absolute values of radius.

Fig. 1 The scheme of PTV algorithm with the correction method.

2.2

Correction over Particle Image Correlation for PTV

The performance of particles detection methods can be appraised according to two capabilities: particles recovery rate and particles center position estimation accuracy. Aforementioned particle mask correlation method is capable of high level of the recovery rate.

To achieve high accuracy a number of algorithms can be employed for particle center subpixel position estimation. The simplest one is "Center of gravity method". More comprehensive methods are: "Three point Gaussian interpolation" and "Two dimensional Gaussian interpolation". However, computation results on test images have shown that detection of the particle center location suffers from inaccuracy and liable to the peak-locking effect. Taking into account that there are two particle center locations forming velocity vector, the error rises.

For the purpose of the error reduction in resulted velocity vector, present work announces a novel Correction over Particle Image Correlation (CPIC) algorithm. The proposed correction is a new step between vector formation and outliers detection. After all, joint action of particle mask correlation method with present correction allows gaining high accuracy with good level of recovery rate.

To perform correction the original particles images on both frames are cross correlated producing the correlation field. The subpixel maximum of the field is the correction vector value. Thus this approach has the same drawbacks with subpixel interpolation as for particle center position estimator. This is true except the fact that the subpixel interpolation is to be done once per vector, while it is applied twice during conventional vector forming. Nevertheless the correction achieved in this manner is insufficient and resulted vector is still exposed by the peak locking effect.

To archive further improvements the original particle images are preliminary reconstructed. Particle image vicinity with non integer coordinates previously obtained by PMC method is interpolated from original image (Fig. 2). Cubical b-spline interpolation scheme was chosen for reconstruction. Resulted images passed through the aforementioned correction procedure. Another advantage of such an approach is that it can be iteratively applied using new particles pair coordinates determined in the previous iteration step.
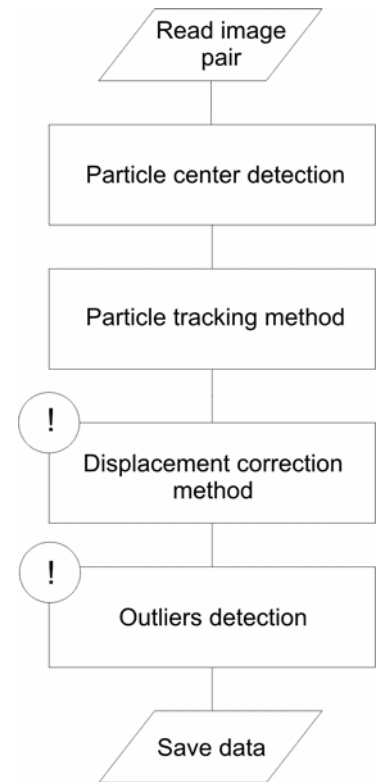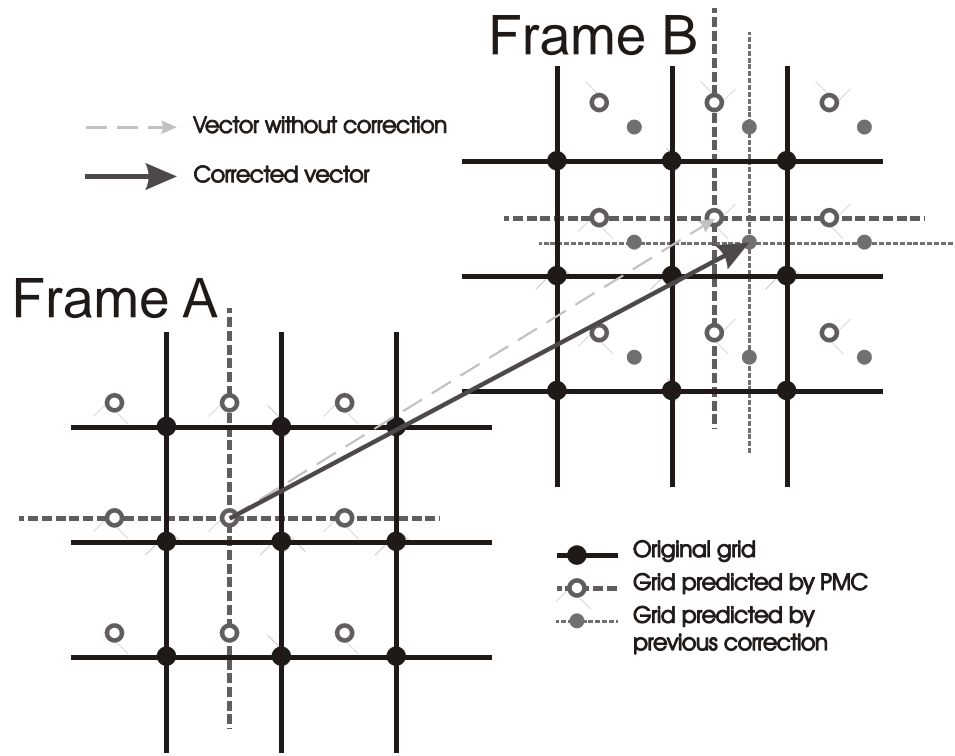
Fig. 2 Scheme of the correction method

2.3
Outliers detection

Automated image processing inevitably leads to an appearance of outliers. Such vectors can appear due to low image quality, high velocity gradients, essential out-of-plane velocity component and other effects. Searching and removing such vectors before subsequent analysis is imperative because their influence can not be eliminated from resulting data.

2.3.1
Moving average algorithm for regular PIV data

The method is based on considerations of local smoothness of velocity field. The value of each vector is compared to its neighboring vectors. The vector $v(x, y)$ is considered as an outlier if the following condition is hold: $\|v(x, y) - \overline{v}(x, y)\| > k$, where $\overline{v}(x, y)$ - an average local velocity over neighboring vectors from vicinity of the vector. The threshold value k is calculated as follows: $k = \alpha \max_{x,y} \|v(x, y) - \overline{v}(x, y)\|$, where $0 < \alpha < 1$.

2.3.2
Moving average algorithm for irregular PTV data

The problem of the application of the moving average algorithm on irregular data is the difficulty of choosing the proper interrogation area, which will definitely contain neighboring vectors. In this case, if we consider the large enough area a fortiori containing vectors, then method will suffer from inaccuracy in flows with high velocity gradients since the average velocity can strongly differ from local velocity. To solve this problem it was proposed to consider large area with appropriate weighting. The Gaussian function was chosen as a weighting function. Thus the original inequations turn into:

$$\|v(r_0) - \overline{v}(r_0)\| > k; \quad \overline{v}(r_0) = \sum_{n \ni N(r_0)} v_n \cdot w_n(r_0) / \sum_{n \ni N(r_0)} w_n(r_0)$$

$$w_n(r_0) = \exp\left\{-\frac{\|r_0 - r_n\|}{2 \cdot \sigma^2}\right\}; \quad k = a \max_{n \ni N(r_0)} \left(\|v_n - \overline{v}(r_0)\| \cdot w_n(r_0)\right)$$

where $N(r_0)$ – is the aggregate of the vectors from the region under consideration. Described method can be applied iteratively several times. Each iteration removes the most different vectors from the locally weighted mean vector.

Adding two more parameters allows overcoming another problem, which become apparent when the velocity vector field is already rather clean. The peculiarity of this method is that it always finds outliers, marking as spurious every vector mostly differing from the average one. New parameters aim to limit the low bound of such a deviation that is sufficient enough to mark vector as spurious. The first parameter is the absolute low bound and the second one is relative to the mean vector length low bound.

3
Tests

3.1
Synthetic image test

The set of synthetic images was generated to test efficiency of the PTV algorithm with proposed CPIC algorithm. Also the comparison of the PTV method was performed to standard and adaptive (miltipass- multigrid) PIV methods. The data from the works by Raffel et al. (1998), Perez. et al. (2005) were considered during the analysis of the comparison results.

Separate test cases were used to evaluate different parts of the proposed algorithm: particle center detection, particle pair matching and overall performance evaluation in terms of mean bias and random errors. Synthetic images were as large as 1024x1024 pix size in order to obtain enough test points. Gray intensity depth was 16bit. The CCD sensor random noise was not modeled. The effect of the out-of-plane particle motions was not taken into account. For all tests considered below except the test on performance of the particle pair matching procedure (Fig. 3, left) the number of particles were chosen to be 20,000 per image (0.019 particles/pix^2).

Particle center detection test was performed through artificial images with the particle image diameter in the range from 1 to 7 pix, step 0.1 pix with Gaussian shaped particle pattern. Particle image diameter D_p was defined by the width of the pattern at the e^{-2} intensity value according to Raffel et al. (1998). Uniform particle displacement $d = 0.5$ pix was generated since the algorithm has maximum error at the fractional half-pixel particle shift.

The result of the random error of the displacement as a function of particle image diameter D_p is presented in the Fig. 3, left. Results for standard PIV and basic PTV have noticeable minima of the random error at D_p =2.5 pix and 1.9 pix, which fits well with Raffel et al. (1998), Westrerweel (2000), Perez et al. (2005). Moreover the curve that corresponds to the PTV results has the second minimum and according to the Perez et al. (2005) there are further minima with an increase of D_p. Application of the CPIC algorithm allows enlarging the range of the particle image diameters for which the error stays relatively small.

The graph, corresponding to CPIC PTV has the similar shape as for adaptive PIV algorithm. In the range 1-1.5 pix both PTV methods show unstable manner. This can be linked with the low frequency particle image filtration during the particle center detection by PMC.
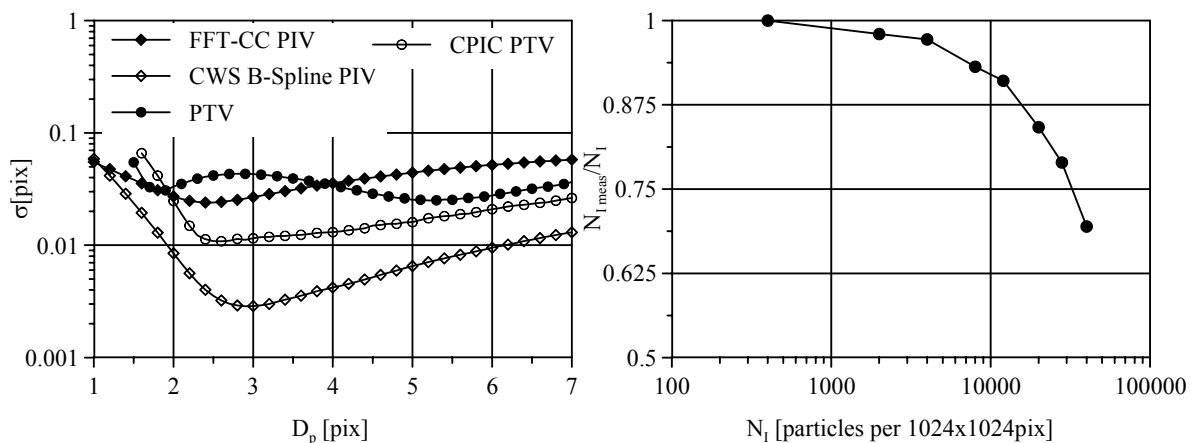

Fig. 3 Random error for synthetic images as a function of the particle image diameter (left) and the number of valid vectors for different particle image concentrations (right)

During the test on particle pair matching method performance the number of paired image particles N_{Imeas} was calculated for different particle concentrations N_I (Fig. 3, right). At low concentrations the number of particle pairs coincides with the number of generated particles. With the increase in concentration up to 4,000 (0.0076 particles/pix^2) the number of found particles becomes different from the origin concentration. At

concentration level 40,000 (0.038 particles/pix^2) 70% of particles are determined. Thus PTV algorithm has upper concentration level at which the efficiency of the particle pair matching decreases.

Algorithm accuracy assessment was done on the base of synthetic images with uniform horizontal shift in the range from 0 to 2 pix, step 0.05 pix. In Fig. 4 mean bias and random errors for PTV and PIV methods are shown. Error graphs have periodic shape depending on imposed displacement (Astarita and Cardone 2005). Displacement uncertainty decreases for CPIC PTV, though remaining bigger than adaptive PIV error level. This can be explained by lower interrogation area size that was used for CPIC algorithm. Also in Fig. 4 two curves are depicted corresponding to the CPIC PTV with 3 and 5 pix sized correlation window in correction procedure.
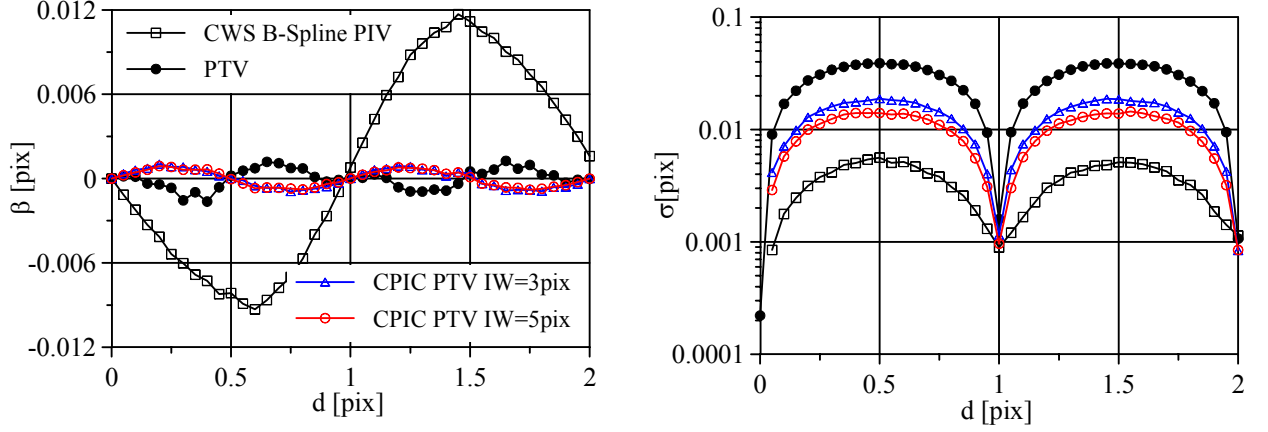

Fig. 4 Mean bias (left) and random (right) errors for synthetic PIV images as a function of the imposed displacement
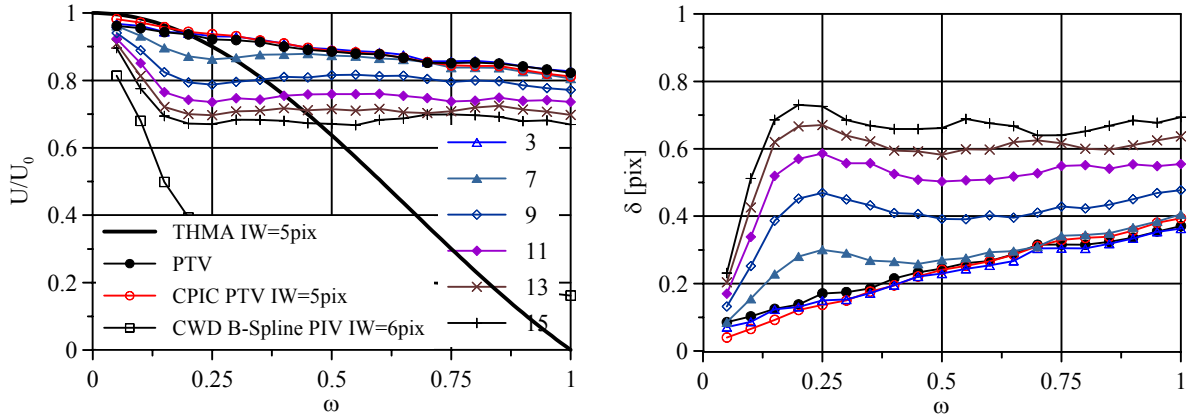

Fig. 5 Spatial frequency response with comparison to top hat moving average filter (THMA) (left) and total error (right) of PIV and PTV algorithms for 1D sinusoidal displacement as a function of imposed spatial frequency

One more synthetic image test was performed to prove that spatial resolution of PTV is conserved after applying CPIC method. Artificial images were generated with 1D sinusoidal displacement and various spatial frequencies for vertical velocity component along x axis: $v = 3\sin(2\pi\omega x/5)$, where $\omega = IW/\lambda = 5/\lambda = 0.05 \div 1$ - spatial frequency, step 0.05 and $IW = 5$ pix - optimal recommended interrogation area size for CPIC algorithm. The measurement transfer function $U/U_0 = T(\omega)$ was calculated for all data points in a velocity field for current spatial frequency

$$\omega: \quad \delta(\omega) = \frac{1}{N}\sum_{i=1}^{N}(U_{0i} - T(\omega)U_{0i})^2; T(\omega) = 1 - \sqrt{\delta(\omega)^2 / \sum_{i=1}^{N}U_{0i}^2}, T(\omega) < 1 \quad \text{(Astarita 2006). In Fig. 5, left, several}$$

modulation transfer functions are presented for the current test: top-hat moving average filter (THMA) and graphs for basic PTV, CPIC PTV with 3, 5, 7, 9, 11, 13, 15 pix interrogation area sizes. The result of THMA filter is used as a reference, which has close behavior to cross-correlation PIV transfer characteristic. Small deviation in MTF results is observed between basic PTV and CPIC PTV with 3 and 5 pix interrogation area size. Curves for other window sizes show lower spatial resolution since they have lower cut-off frequency. The prevalence of the 5 pix window size compared to 3 pix could be seen in Fig. 4, right, where rms uncertainty is lower for the 5 pix window size. So the optimal parameter of correlation window size is found to be 5 pix. For $\omega < 0.5$ in Fig. 5, left, CPIC PTV method gives slightly better accuracy while at the rest part of the graph it shows insignificant degradation of the resolution. Total error results in Fig. 5, right, justify this tendency. Thus CPIC algorithm with small interrogation

window which contains few particles almost does not degrade the locality of the PTV method.

3.2
Experimental test

The efficiency of the proposed method is also demonstrated on the base of several tests on laboratory flows, including different configurations of free and confined jets.

3.2.1
Case A PIV Challenge 2003

In addition to synthetic tests the real images from the case A, PIV Challenge 2003 (Stanislas et al. 2005) were processed. Experimental flow structure in this case is the ax symmetric turbulent jet in stagnant surrounding with $Re=2,000$. The aim of this test here was to verify proposed CPIC PTV method on the intensity of the bias error linked with peak-locking effect. In Fig. 6 the PDF of the axial velocity component is presented for two methods: basic PTV and CPIC PTV. Also the result of the adaptive PIV method is plotted as a reference. The result of the basic PTV procedure shows rather big systematic error. The proposed method allows decreasing this error to the level even lower than for adaptive PIV. The presence of the severe bias error for the basic method can be accounted for low particle image diameter of the test images, which was of the order of one pixel as reported by Stanislas et al. (2005). At this size, 3 point Gaussian subpixel fit has significant bias (Raffel et al. 1998). In the basic PTV method, measured displacement is obtained by calculation of the distance between two positions of particles which are assessed by two independent subpixel evaluations. That is why the bias is quite big. Bias error can be decreased by the shift of the correlation maximum position toward zero values, in the way of reducing the shift to the level lesser than 0.5 pix. This effect can be achieved by continuous window shift technique used in PIV.
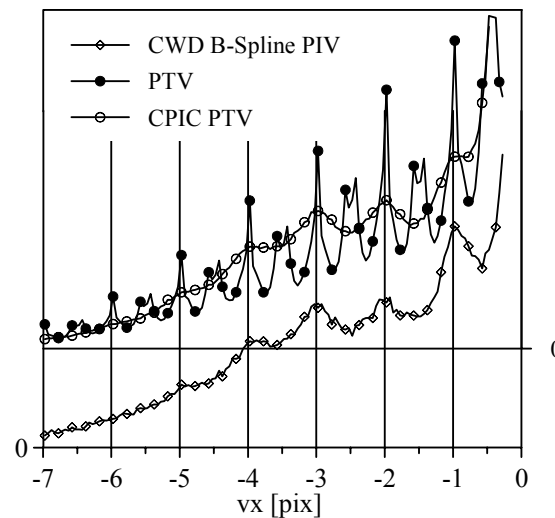
Fig. 6 Probability density distribution of the axial velocity component in a free jet (PIV Challenge 2003, Stanislas M. et al. 2005)

3.2.2
Test on turbulent axisymmetric impinging jet

3.2.2.1
Experimental setup parameters

Experimental setup was prepared to investigate the characteristics of submerged impinging jet. Obtained particle images are used to test the present CPIC method. Jet flow was organized within rectangular transparent Plexiglas tank 40 cm height, 20 cm width and 20 cm length. During experiment the temperature of the water was kept on the constant level by the thermostat and was equal to 32±0.5˚C. Experiment was carried out for turbulent flow regime with $Re=19,000$, which was defined on the basis of mean flow rate velocity $U_0=1.028$ m/s and profiled nozzle diameter $d_{nozzle}=15$ mm. The nozzle was located at the distance of 3 nozzle diameter to the impinging surface. Nd:YAG laser "NewWave Solo III" with 50 mJ pulse energy was used to illuminate flow field. Laser sheet was formed by cylindrical lens. The width of the laser sheet in the studied region was 0.8 mm. To register particle images "POLIS" CCD digital camera with 1360×1024 pix^2 resolution ratio and 10 bit capacity was employed. Traversing mechanism handled the positioning of the camera. There were two experiments performed with different sizes of the measuring area: 35×25 mm^2 and zoomed area 6.5×5 mm^2. In the first experiment water was seeded with 20 μm polyamide particles and for the second experiment – 5 μm particles were used. Density of the particles

was 1.05 kg/m^3. In both cases upper bound of measuring area coincided with the edge of the impinging surface. During the experiment 3,000 images were acquired in order to extract reliable statistics information.

3.2.2.2
Processing parameters

Experimental data was processed by Relaxation PTV with and without CPIC algorithm application. Besides the results from miltipass- multigrid adaptive PIV processing were compared with PTV results. Image preprocessing was applied before particle image displacement calculation. Impinging wall appeared at the top part of an image was masked with zero intensity padding. Furthermore the average gray value field was subtracted from each of the experimental images.

Parameters applied for the first experiment with large measurement area are listed below. Particles seeding density was about 20,000 particles per image (0.02 particles/pix^2).

Hybrid Relaxation method was applied with T_n = 15 pix, T_q = 3 pix, 3 passes. Predicted area radius was within the range of [5; 8] pix with the ratio R = 0.5. CPIC algorithm was applied with 5 pix sized correlation window, 4 passes. Subsequent outliers detection was performed with averaging radius R_{avrg} = 20 pix and weighting Gauss sigma σ_{wght} = 10 pix, α = 0.99, 2 passes, absolute low bound – 1 pix and relative low bound – 10 %. Statistics was obtained using original irregular data without interpolation.

Final resolution for PIV was chosen at IW = 16 pix with grid point distance 8 pix (50% overlapped windows). Initial interrogation area size was IW = 32 pix. Two iterations of CWD PIV were made with initial IW size and then after grid refinement two more steps were processed with final resolution. Between iterations the procedure of vector field outlier detection was applied similar to those described in Westerweel, Scarano (2005), and all outliers were replaced by interpolated vectors. After last iteration the vector replacement was not performed. During cross-correlation calculation, image interrogation areas were weighted by 2D Gauss window function with the half-height width of 0.5 IW in order to increase effective spatial resolution. Third order b-spline interpolation scheme was used for image deformation.

Second experiment for zoomed measurement area with seeding density about 7,500 particles per image area (0.007 particles/pix^2) was processed with the following parameters.

For hybrid Relaxation PTV the neighborhood radius T_n was of 15 pix. Minimum and maximum radiuses of predicted area were 2 and 8 pix respectively. The parameters for outliers detection were the following: averaging radius R_{avrg} = 20 pix and weighting Gauss sigma σ_{wght} = 15 pix, α = 0.99, 1 pass, absolute low bound – 0 pix and relative low bound – 20 %. Other parameters were the same as in previous experiment.

PIV interrogation was performed with the same parameters as for the first experiment except of the window size which was two times larger, i.e. IW =64 pix and IW =32 pix for starting and final window sizes respectively.

3.2.2.3
Experimental results

This part of the work contains statistical characteristics for impinging jet. In Fig. 7 the instant velocity field for the low-resolution experiment and zoomed experiment are presented. Further results, shown in Figs 8-11, are graphed along cross-sections depicted with black lines in Fig. 7.

In Fig. 8 the horizontal profiles of mean velocity are depicted. The jet axis of symmetry corresponds to zero value of the abscissa axis. The maximum velocity at the nozzle exit is V_y =1.028 m/s. All curves corresponding to mean velocity in Fig. 8 show good coincidence. The exception is the PIV result for the range from r/D = 0.2 to 0.45 in a mixing layer, where maximum deviation from PTV result reaches 4 %. This can be linked with velocity spatial averaging inherent in PIV processing.

Turbulent intensities of radial (V_x) and axial (V_y) velocity components in horizontal cross-section are shown in Fig. 9. Major distinctions between second order moments calculated by different methods are observed in the center of shear layer where pulsations have maximum. It is seen that PTV results are higher than PIV results. This behavior can be explained both by error level for concrete PTV/PIV algorithm and by effect of spatial resolution which depends on size of the measurement area, size of the interrogation area for PIV and mean distance between detected particles for PTV (E. A. Cowen, S. G. Monismith 1997).

The inaccuracy of an algorithm dominantly impacts on measured turbulence intensity in experiment with high optical resolution (small measurement area). At the same time both an error and spatial resolution issues of the method have approximately equal influence on measured turbulence intensity for experiment with low optical resolution (large measurement area). It is known that increasing of algorithm error leads to the rise of the velocity second order moments and vice versa. Refinement of spatial resolution, up to several Kolmogorov lengthscales

(Saarenrinne et al. 2001), also leads to raising of measured magnitude of turbulence intensity. Last tendency is explained by limited transfer function of the digital image velocimetry at high spatial frequencies and also by the limitation of the turbulence energy spectrum at high spatial wave numbers.
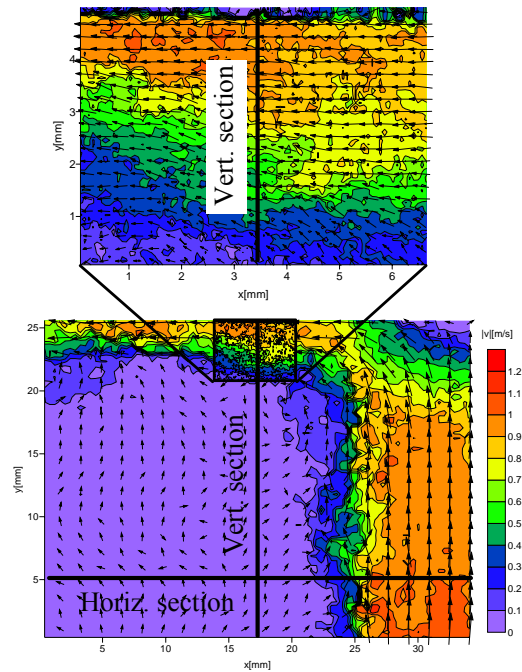

Fig. 7 Typical instantaneous velocity fields for both experiments and chosen cross-sections
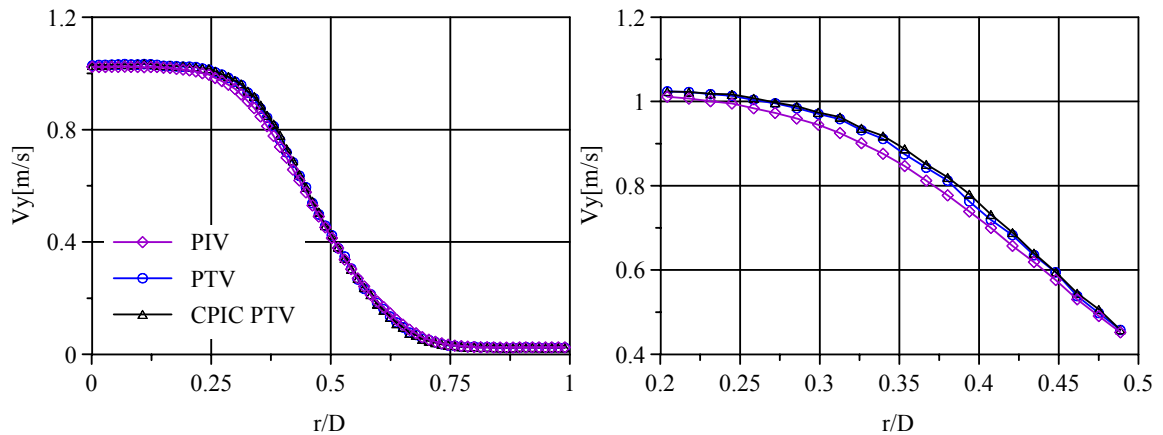

Fig. 8 Mean velocity horizontal profile (*y*=5mm) for streamwise velocity component calculated by different methods (left) and zoomed (right), large area.
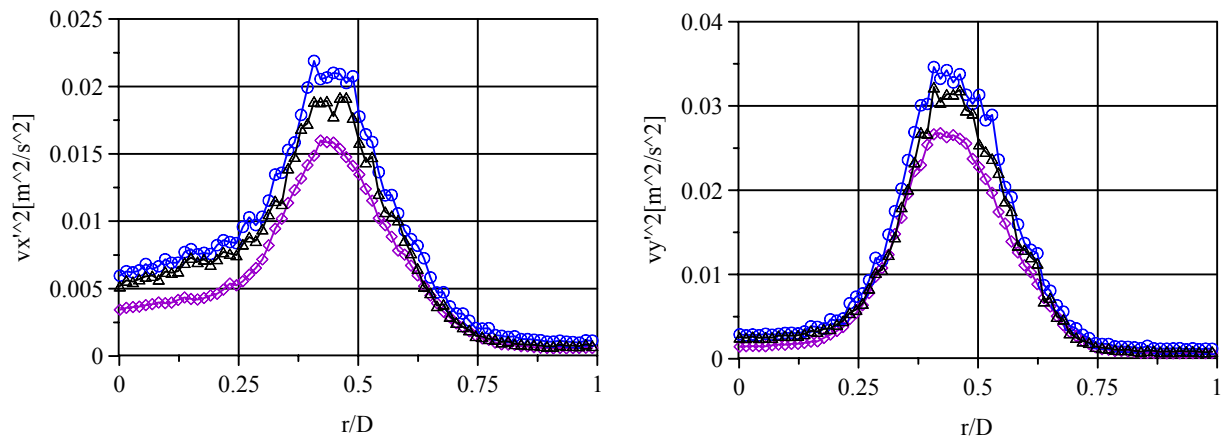

Fig. 9 Second order velocity moments in horizontal cross-section (*y*=5mm) for radial velocity component (left) and streamwise velocity component (right) calculated by different methods, large area.

The distributions of velocity components shown in Fig. 10 refer to the near wall measurements. Here first and second order velocity moments are shown for high and low optical resolution experiments. In Fig. 10 the mean velocity profiles are presented in logarithmic scale with high detailing near impinging wall. Statistics for PTV data was calculated on 16 pix grid and grid step for PIV was equal to 16 pix ($IW = 32$ pix with 50 % overlap). Difference between PIV and PTV profiles in Fig. 10, left, for y'= 0.2 mm was of 3% and can be related with velocity underestimation by PIV due to high velocity gradient in this region.
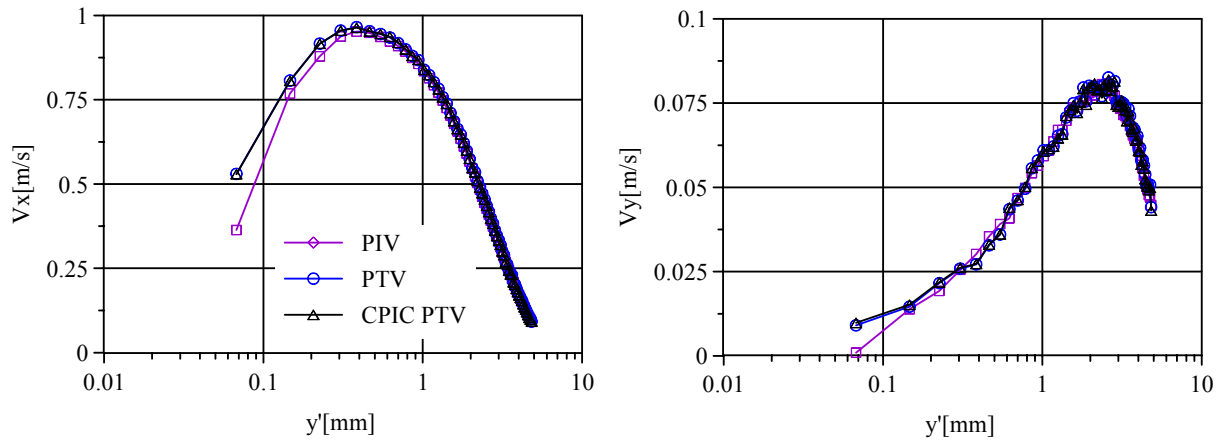

Fig. 10 Mean velocity vertical profile (x=3,4mm) for streamwise velocity (left) and normal to the wall velocity (right) calculated by different methods, zoomed area

In Fig. 11 the profiles of second order velocity moments are shown for vertical cross-section. In this graph the results are presented for basic PTV, CPIC PTV and adaptive PIV for both low and high optical resolution. As it is seen, curves corresponding to PTV processing have similar level of velocity fluctuations as compared to PIV with high optical resolution. It can be concluded that PTV algorithms allow to resolve fine velocity fluctuation scales even for low optical resolution, in contrast to the adaptive PIV, which underestimates the fluctuation level at such conditions. Also, the second order moments far from the wall (y'>5 mm) are of particular interest. The flow in this area expected to have near zero velocity and velocity fluctuations. It is seen that PIV and CPIC PTV results lay close to each other, whereas basic PTV results have higher rms uncertainty especially for V_y' (Fig. 11, right), that confirms the error reducing by proposed method.
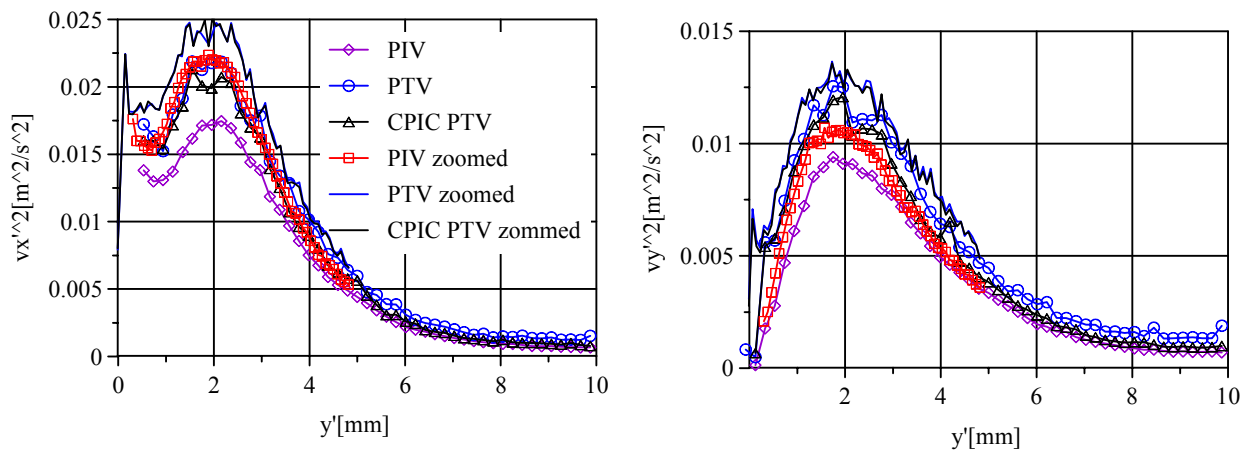

Fig. 11 Second velocity moment vertical profile (x=3.4mm) for streamwise velocity (left) and normal to the wall velocity (right) calculated by different methods, zoomed area

4
Conclusion

In this paper a novel Correction over Particle Image Correlation (CPIC) algorithm is announced. Proposed correction can be applied to calculated irregular PTV velocity field using the original particle images.

CPIC algorithm was tested on synthetic images. The influence of the particle image parameters to the correction value was investigated during tests and optimal parameters were proposed. It was shown that employing the CPIC algorithm allows a wider range of particles diameters to be used while the error level remains rather low. The results of the test with uniform particles displacement indicate three times total error reduction.

Applying the correlation based correction procedure is expected to degrade the spatial resolution which is not

always the case. Using proper correlation window size one can choose between accuracy and spatial resolution. According to the results, it is optimal to use 5 pix correlation correction window size for conventional PIV image with 0.02 particles/pix^2 density without any spatial resolution penalty.

Two experiments on impinging jet were performed. First one embraces whole flow evolution. Second experiment allowed to test the flow near the wall with high optical resolution and was intended to control the spatial resolution of studied methods. Statistical turbulence characteristics of the flow near the impinging wall were investigated by basic PTV, CPIC PTV and also by PIV.

Described approach manifested its advantages on the base of real experiments. Remarkable result of applied CPIC algorithm is its ability to reduce the peak-locking effect to the level of one of the adaptive PIV.

Extended spatial resolution of the PTV approach comparing to the PIV was confirmed and it was shown that proposed correction doesn't worsen the locality of the method, reducing the error level. Thus CPIC PTV approach provides both accuracy and spatial resolution.

Acknowledgements

References

Astarita T; Cardone G (2005) Analysis of interpolation schemes for image deformation methods in PIV. Exp. Fluids, 38, 233–243

Astarita T (2006) Analysis of interpolation schemes for image deformation methods in PIV: effect of noise on the accuracy and spatial resolution. Exp. Fluids, 40, 977–987

Baek S.J.; Lee S.J. (1996) A new two-frame particle tracking algorithm using match probability. Exp. Fluids, 22, 23–32

E. A. Cowen, S. G. Monismith (1997) A hybrid digital particle tracking velocimetry technique. Exp. Fluids, 22, 199–211

Etoh T.; Takehara K. (1998) The particle mask correlation method. Proc. 8th Int. Symp. on Flow Visualization # 283

Pentti Saarenrinne, Mika Piirto and Hannu Eloranta (2001) Experiences of turbulence measurement with PIV*, Meas. Sci. Technol. 12 1904–1910

Raffel M., Willert C., Kompenhans J. (1998) Particle image Velocimetry. A practical guide, Berlin: Springer.

Scarano F. (2002) Iterative image deformation methods in PIV. Review article. Meas. Sci. Technol., 13, R1-R19

Stanislas M.; Okamoto K.; Kahler C.J. (2005) Main results of the Second International PIV Challenge. Exp. Fluids, 39, 170–191

Westerweel J.; Scarano F. (2005) Universal outlier detection for PIV data. Exp. Fluids, 39, 1096–1100